SUPPORTING INFORMATION

FOR

Hydrophobic association and ionic coordination synergistically enhance a multifunctional hydrogel for high-performance wearable strain sensing

Jiayi Fu [a], ChengRui Jiang [a], Wanping Xiang [a], Guangtao Chang [a,b,*], Ruoxin Li [a,b,*]

[a] College of Textile and Clothing Engineering, Soochow University, Suzhou 215123, PR China

[b] Jiangsu Engineering Research Center of Textile Dyeing and Printing for Energy Conservation, Discharge Reduction and Cleaner Production (ERC), Soochow University, Suzhou 215123, PR China

[*] E-mail: liruoxin@suda.edu.cn (Ruoxin Li), changgt@suda.edu.cn (Guangtao Chang)

Contents

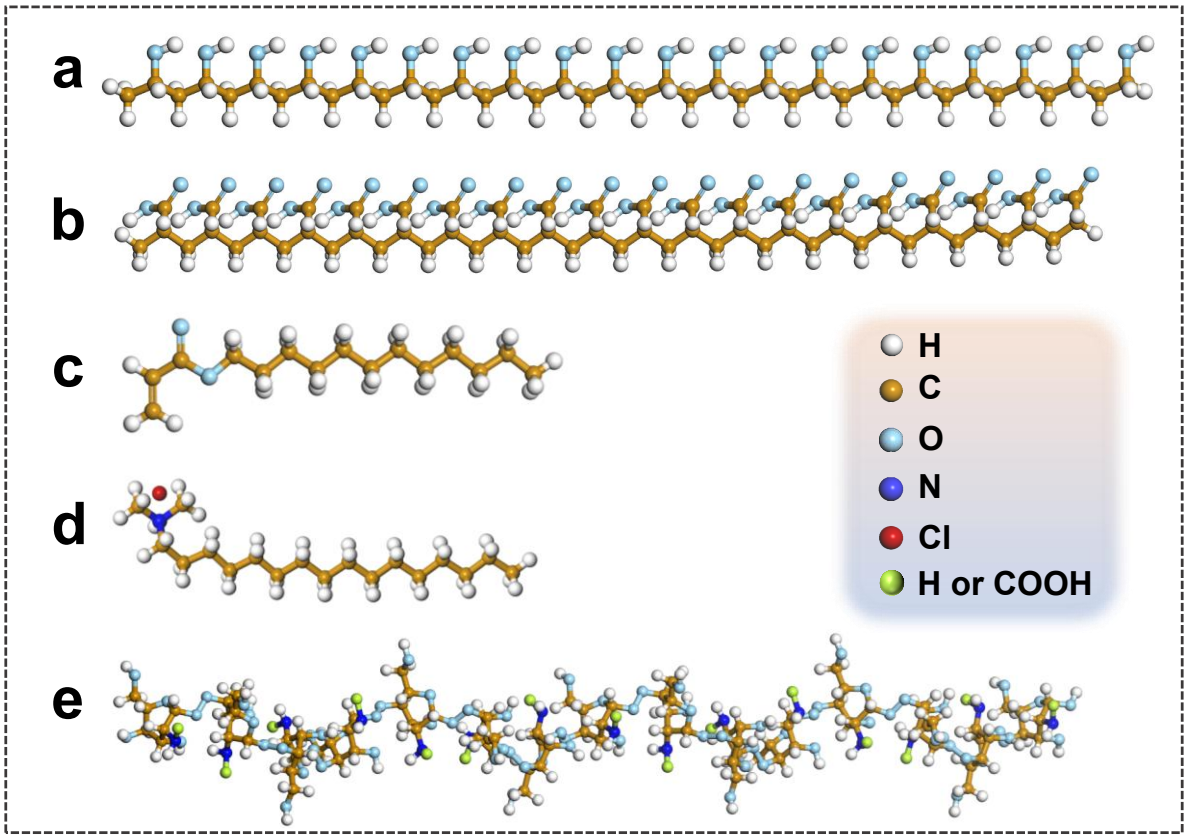

Figure S1. The structural formula of the main components in the hydrogel: (a) PVA, (b) PAA, (c) LA, (d) CTAB, (e) CS. The elements represented by each ball are labeled in the figure.

Part S1. Preparation of Hydrogel

All hydrogel precursors were homogeneously mixed according to the mass ratios listed in Table S1. After thorough agitation to ensure uniform dispersion, the mixture was centrifuged at 2000 rpm for 2 minutes to remove all air bubbles. The degassed solution was then transferred into appropriate molds and subjected to crosslinking at 60 °C for 6 hours in a sealed environment. Finally, the corresponding hydrogels were obtained.

Table S1. Material composition of PA, PALC, and PALCC hydrogels.

Sample	PA	PALC	PALCC
AA	1.5	1.5	1.5
PVA solution	3	3	3
DES	3	3	3
LA	/	1.5	1.5
CTAB	/	0.2	0.2
CS solution	/	/	0.75
MBA	0.01125	0.01125	0.01125
APS	0.018	0.018	0.018

Note S1: The mass unit of each material in the table is ***g***.

Part S2. Characterization

S2.1 Morphology and Structural Composition

The surface morphology of the hydrogels was examined using a high-resolution field-emission scanning electron microscope (SEM, Regulus 8100, Hitachi, Japan). Prior to observation, the samples were immersed in deionized water for 24 h to replace the glycerol phase. The swollen hydrogels were subsequently frozen at -50 °C for 24 h and vacuum-dried for 48 h to remove all residual water. After drying, the samples were fractured in liquid nitrogen to obtain a clean cross-section, sputter-coated with gold, and then observed under the SEM. The elemental composition of the hydrogels was analyzed using an energy-dispersive X-ray spectrometer (EDS, TM3030, Hitachi, Japan).

The chemical structure of the hydrogels was characterized using Fourier transform infrared spectroscopy (FTIR, NICOLET iS5, Thermo Fisher Scientific, USA). The freeze-dried hydrogel powders were finely ground and mixed with KBr at a mass ratio of 1:150, followed by pellet pressing. Spectra were recorded in the range of 4500-500 cm^{-1}.

The particle size evolution of hydrogels during the high-temperature crosslinking process was analyzed using dynamic light scattering (DLS, Zetasizer Nano ZS90, Malvern Panalytical, UK). Measurements were performed in disposable polymethyl methacrylate cuvettes with a light path length of 10 mm. Each sample was tested three times at each crosslinking stage, and the average values were reported.

Small-angle X-ray scattering (SAXS, SAXSess MC2, Anton Paar, Austria) was employed to investigate the formation of micellar structures within the hydrogels.

S2.2 Mechanical Properties

The mechanical properties of the hydrogels were evaluated using a universal testing machine (KY-D2503, Shanghai Horiba Precision Instrument Co., Ltd., China). For tensile tests, dumbbell-shaped specimens were prepared according to the Chinese National Standard Type II mold, with an effective gauge length of 25 mm and a tensile rate of 50 mm min^{-1}. For compression tests, cylindrical samples (5 mm in height and 20 mm in diameter) were tested

at a compression rate of 10 mm min^{-1}. Each sample shall be tested at least 5 times.

S2.3 Rheological Properties

The rheological behavior of the hydrogels was analyzed using an advanced rotational rheometer (DHR-2, TA Instruments, USA) equipped with a 20 mm parallel-plate geometry. The gap between plates was maintained at 1 mm, and the temperature was controlled at 25 ± 0.5 °C. Small-amplitude oscillatory frequency sweep tests were performed in the angular frequency range of 0.1-100 rad s^{-1} at a fixed strain amplitude of 0.1%.

S2.4 Environmental Stability

(1) Anti-drying Performance

The anti-drying performance of the hydrogels was evaluated by placing the samples in a constant temperature and humidity chamber at 25 °C and 50% relative humidity (RH). The samples were weighed every 24 h, and the test continued until the mass change reached equilibrium. For each type of hydrogel, three specimens were tested, and the average value was reported.

The weight retention ratio (WRR) was calculated using **Equation (S1)**:

$$WRR = \frac{W_t - W_0}{W_0} \times 100\% \quad \text{(S1)}$$

where WRR represents the weight retention ratio (%), W_t is the real-time weight of the sample (g), and W_0 is the initial weight of the sample (g).

(2) Anti-swelling Performance

Prior to the swelling test, the hydrogel samples were equilibrated at 25 °C and 50% RH for 24 h. The samples were then immersed in deionized water at room temperature to allow swelling. At 24 h intervals, the samples were removed, the surface water was gently blotted, and the samples were immediately weighed. Three replicates were tested for each hydrogel type, and the results were averaged.

The equilibrium swelling ratio (ESR) was calculated using **Equation (S2)**:

$$ESR = \frac{W_e - W_0}{W_0} \times 100\% \quad \text{(S2)}$$

where ESR represents the swelling ratio (%), W_e is the equilibrium weight of the swollen

sample (g), and W_0 is the initial dry weight (g).

S2.5 Low-Field Nuclear Magnetic Resonance (LF-NMR)

Low-field nuclear magnetic resonance (LF-NMR, PQ001, Niumag Electronic Technology Co., Ltd., Shanghai, China) was employed to analyze the water distribution and binding states within the hydrogels. Before testing, non-magnetic NMR sample tubes containing deionized water and the three hydrogel samples were equilibrated at 32 °C for 30 min. The experiments were conducted at 32 ± 0.01 °C with a total measurement time of 5000 ms and four accumulations. The transverse relaxation time (T_2) signals were obtained and inverted using the non-negative least squares (NNLS) method to derive the T_2 relaxation time distribution curves.

S2.6 Antibacterial Performance

The antibacterial performance of the hydrogels was evaluated using a shaking flask method. *Escherichia coli* (Gram-negative) and *Staphylococcus aureus* (Gram-positive) were selected as the representative bacterial strains. The PA hydrogel was used as the control sample, while PALC and PALCC hydrogels served as test samples.

Prior to testing, all samples and containers were sterilized in an autoclave at 121 °C for 30 min. The sterilized hydrogel samples were then immersed in the bacterial suspensions and shaken in an incubator for 18-24 h to ensure sufficient contact between the samples and the bacteria. The initial bacterial concentrations were approximately 2.12×10^4 CFU mL^{-1} for *E. coli* and 2.48×10^4 CFU mL^{-1} for *S. aureus*. After incubation, the bacterial suspensions were serially diluted with phosphate-buffered saline (PBS), and 1 mL of each dilution was plated on sterile agar. After the agar solidified, the plates were incubated in an inverted position under constant temperature and humidity conditions for 24-36 h. The colony-forming units (CFUs) were counted once the colonies reached measurable size. The antibacterial efficiency (Y) was calculated according to **Equation (S3)**:

$$Y = \frac{W_t\text{-}Q_t}{W_t} \times 100\% \quad \text{(S3)}$$

where Y represents the antibacterial efficiency (%), W_t denotes the number of colonies in the

control sample (CFU mL^{-1}), and Q_t denotes the number of colonies in the test sample (CFU mL^{-1}).

S2.7 Electrical and Strain-Sensing Properties

(1) Electrical Conductivity

The electrical conductivity of the hydrogels was measured using a digital multimeter (Fluke 17B+, Fluke Testing Instruments Co., Ltd., Shanghai, China). The conductivity (σ) was calculated according to **Equation (S4)**:

$$\sigma = \frac{1}{\rho} \tag{S4}$$

where ρ represents the resistivity of the hydrogel (Ω·m), and σ represents the electrical conductivity (S m^{-1}).

(2) Tensile Strain-Sensing Performance

Rectangular hydrogel samples (50 mm × 15 mm × 2 mm) were prepared, with aluminum foil attached to both ends as electrodes to form a hydrogel-based strain sensor. The effective sensing length of the device was 30 mm. The tensile tests were conducted using a flexible electronic testing system (Prtronic, Mifang Technology, China) at a stretching rate of 1 mm s^{-1}. The real-time current responses under a constant voltage of 1 V were recorded using an electrochemical workstation (CHI760E, CH Instruments Inc., USA).

The strain sensitivity of the hydrogel sensors was evaluated using the gauge factor (*GF*), which was calculated according to **Equation (S5)**:

$$GF = \frac{\Delta R/R_0}{\varepsilon} \tag{S5}$$

where R_0 is the initial resistance of the hydrogel, ΔR is the change in resistance during deformation, and ε is the applied strain.

(3) Compressive Strain-Sensing Performance

Cylindrical hydrogel samples (20 mm in diameter and 5 mm in height) were prepared, with aluminum foil electrodes attached to the top and bottom surfaces to fabricate compressive strain sensors. Cyclic compression tests were performed using a universal testing machine (KY-D2503, Shanghai Horiba Precision Instrument Co., Ltd., China), and

the corresponding electrical signals were simultaneously recorded by the electrochemical workstation.

The compressive sensitivity of the hydrogels was characterized using the gauge factor (*GF'*), calculated as shown in **Equation (S6)**:

$$GF' = \frac{\Delta I / I_0}{\varepsilon} \quad \text{(S6)}$$

where I_0 is the initial current, ΔI is the change in current during compression, and ε is the applied strain.

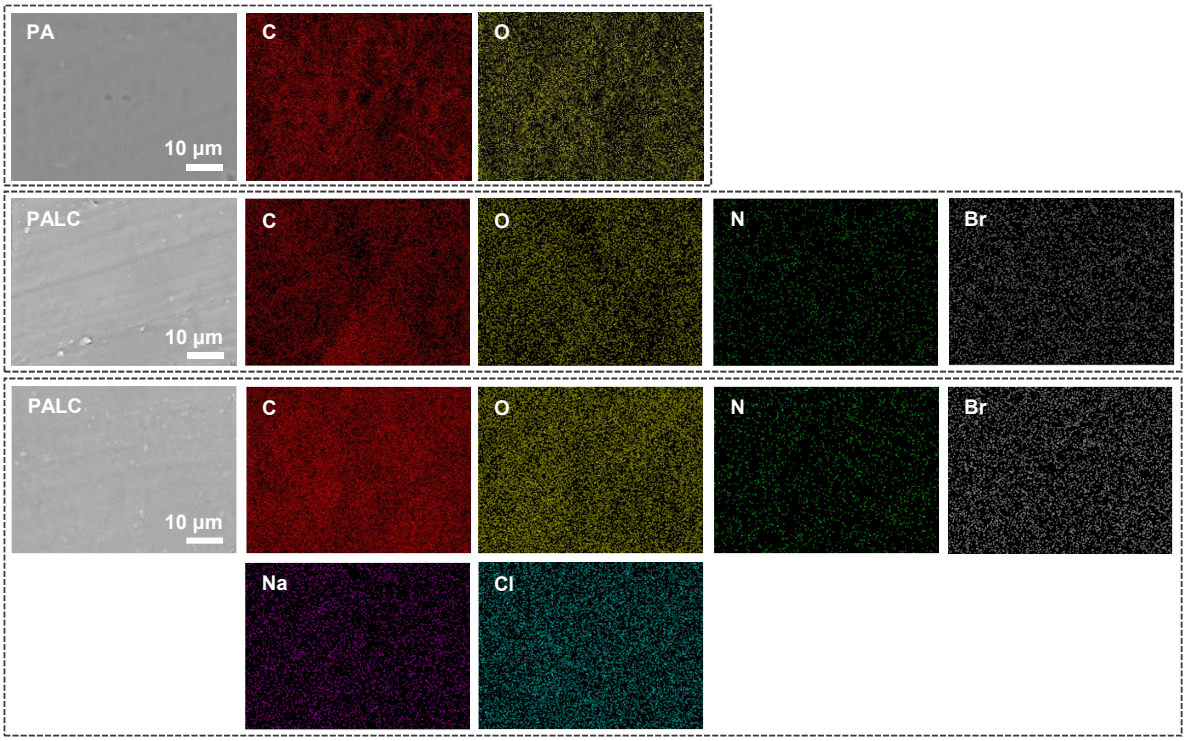

Figure S2. EDS spectrum of PA, PALC and PALCC hydrogel.

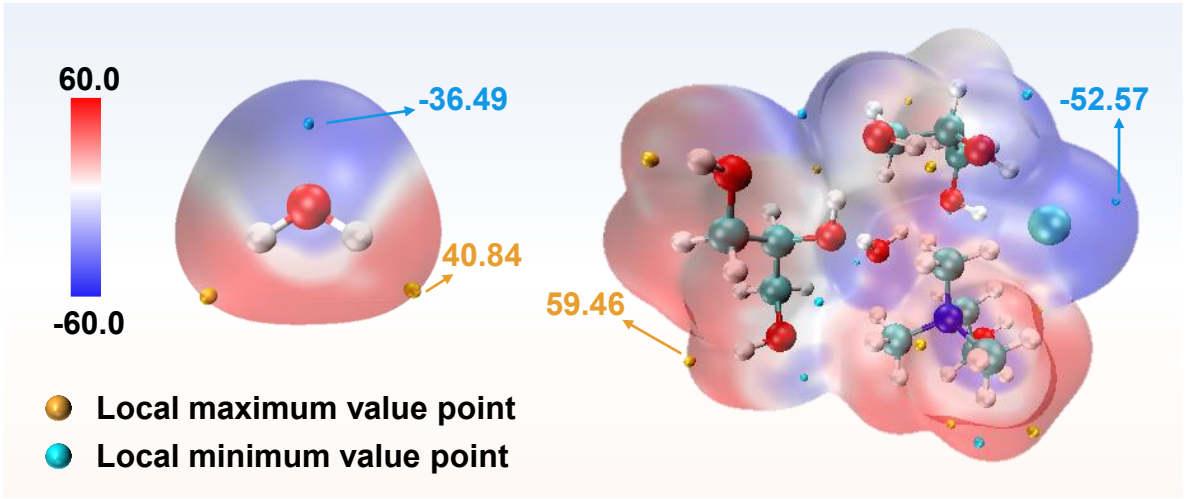

Figure S3. The electronegativity of DES-H_2O system compared with H_2O.

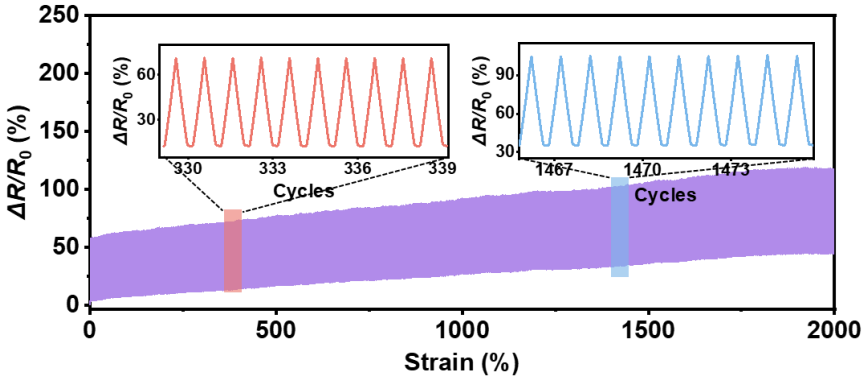

167

168 **Figure S4.** Cyclic curve of PALCC hydrogel sensor under 100% strain loading unloading

169 2000 times in initial state.

170

171

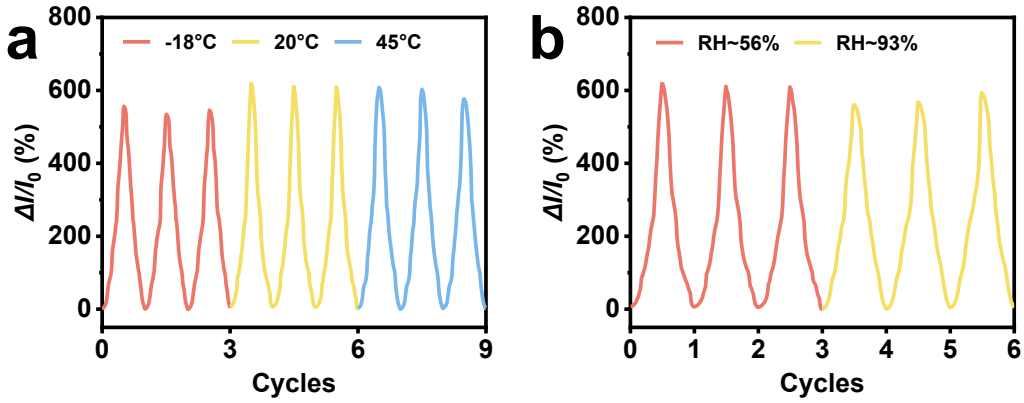

172

173 **Figure S5.** The compressive strain sensing performance of palcc hydrogel sensor in extreme

174 environments: (a) extreme temperature, (b) extreme humidity.

Table S2. The relative percentage of relaxation time value and relaxation peak area of deionized water and hydrogel.

Sample	Relaxation time (ms)			Relative percentage of relaxation peak area (%)		
	T_{21}	T_{22}	T_{23}	T_{21}	T_{22}	T_{23}
H_20	0.00	0.00	2947.37	0.00	0.00	99.83
PA	2.28	251.59	0.00	14.66	85.34	0.00
PALC	2.63	175.20	3406.44	15.02	84.83	0.15
PALCC	3.04	251.59	0.00	13.41	86.59	0.00

Table S3. The basic performance comparison table of recent hydrogel strain sensors.

Materials	Stress (kPa)	Strain (%)	GF (strain range)	Cycle durability	Ref.
PVA/AA/LA/CTAB/CS	296.4	434.6	1.67 (110-270%)	> 2000	This work
NIPAAm/AM/PVP/TA	~ 5	720	3.61 (0-300%)	500	[1]
PVA/Gly/$FeCl_3$	~ 174.62	310	9.21 (310%)	-	[2]
HA/CS/$AlCl_3$	7.7	2100	4.42 (450-800%)	300	[3]
AA/SA/ ethylenediamine / gelatin/$AlCl_3$	99.6	578	~ 1.47 (200%)	-	[4]
PABMA/PVA	596	260	1.5 (50%)	-	[5]
Allyl cellulose /AA	104.67	141.86	0.26 (0-100%)	1000	[6]
SA/$CaCl_2$	1550	160.9	4.0 (100-180%)	330	[7]
PVA/CNF/ borax /DA	~ 270	~ 500	0.13 (0-125%)	~ 60	[8]

Note S2: NIPAAm stands for isopropylamine, am for acrylamide, PVP for polyvinylpyrrolidone, TA for tannic acid, Gly for glycerol, ha for hyaluronic acid, psbma for poly [(2- (methylpropoxy) ethyl) dimethyl] - (3-sulfonopropyl), SA for sodium alginate, CNF for cellulose nanofibers, DA for dopamine hydrochloride.

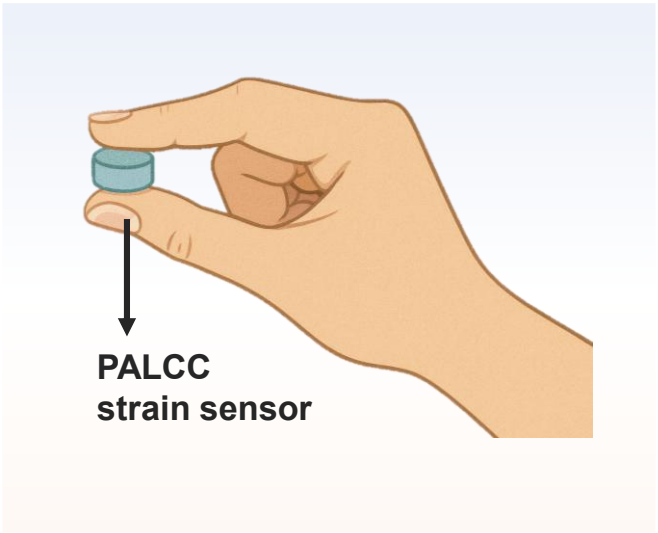

Figure S6. Schematic diagram of cylindrical PALCC hydrogel sensor fixed on fingertips.

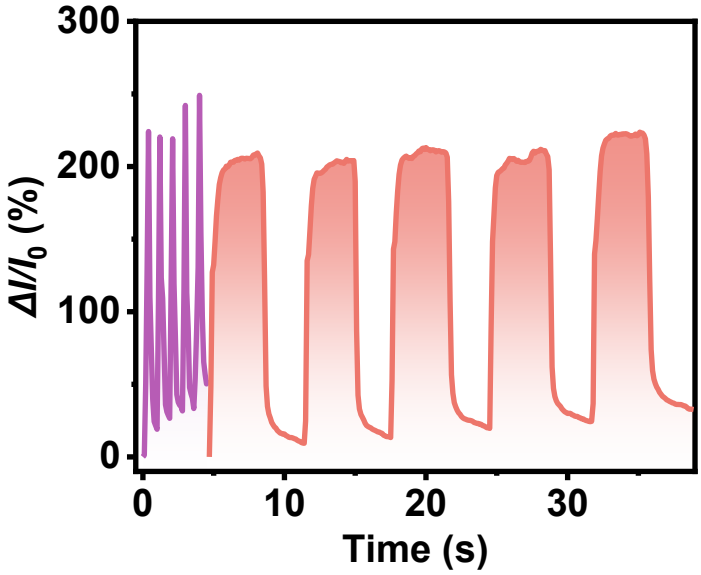

Figure S7. The signal peaks generated by touching and pressing the PALCC sensor.

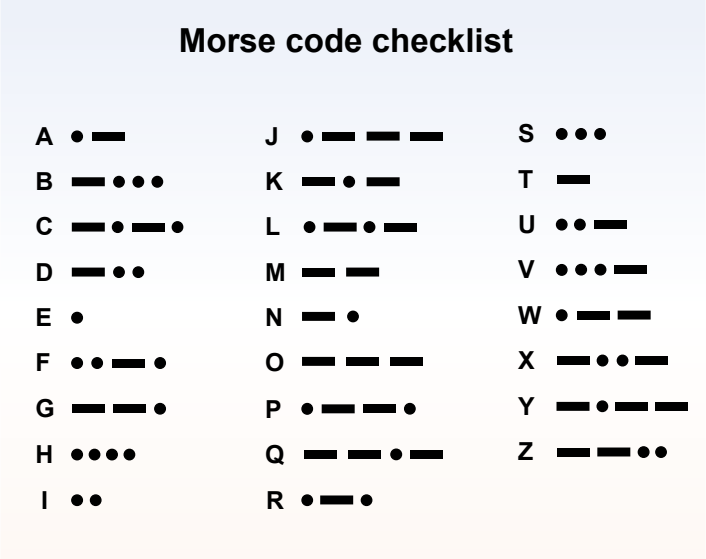

Figure S8. Morse code comparison table.

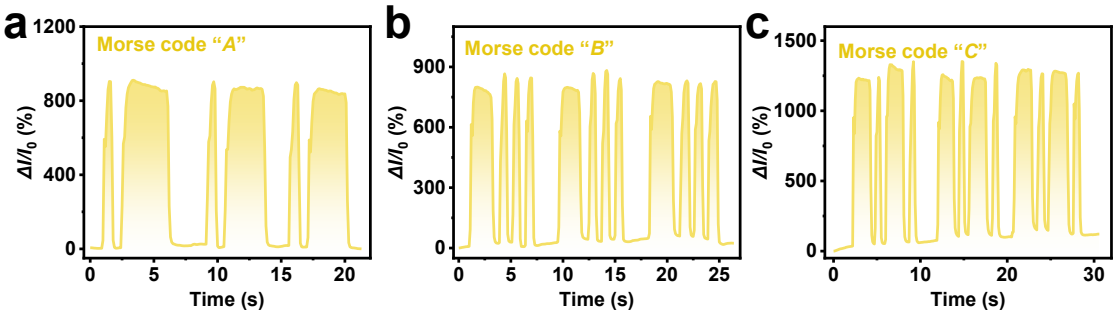

Figure S9. Use Morse code to output the letters: (a) A, (b) B, and (c) C.

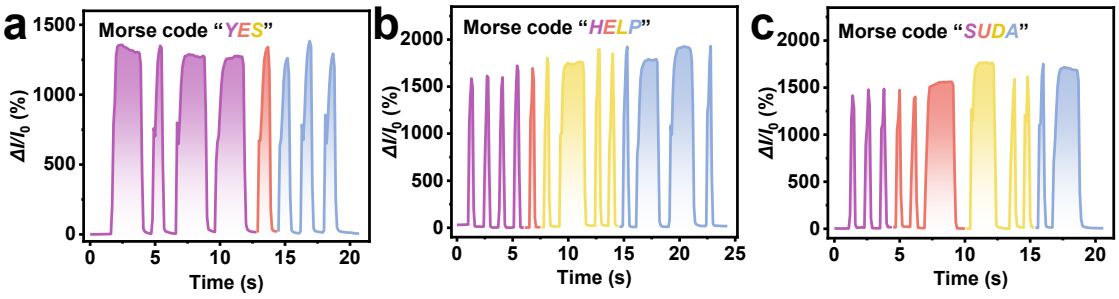

Figure S10. Use Morse code to output words: (a) YES, (b) HELP, and (c) SUDA.

References

1 Pang, Q., Hu, H., Zhang, H., Qiao, B. & Ma, L. Temperature-Responsive Ionic Conductive Hydrogel for Strain and Temperature Sensors. *ACS Appl. Mater. Interfaces*, 26536-26547, doi:10.1021/acsami.2c06952 (2022).

2 Zhao, W. *et al.* Road Narrow‐Inspired Strain Concentration to Wide‐Range‐Tunable Gauge Factor of Ionic Hydrogel Strain Sensor. *Adv. Sci.* **10**, 2303338, doi:10.1002/advs.202303338 (2023).

3 Gao, M., Zhao, R., Kang, B., Zhao, Z. & Song, S. High-performance ionic conductive double-network hydrogel enabling a long-term flexible strain sensor. *Colloids Surf. Physicochem. Eng. Aspects* **663**, 131051, doi:10.1016/j.colsurfa.2023.131051 (2023).

4 Zhao, L. *et al.* Multifunctional Ionic Conductive Double-Network Hydrogel as a Long-Term Flexible Strain Sensor. *ACS Appl. Polym. Mater.* **3**, 5494-5508, doi:10.1021/acsapm.1c00805 (2021).

5 Wang, Z. *et al.* Flexible and wearable strain sensors based on tough and self-adhesive ion conducting hydrogels. *J Mater Chem B* **7**, 24-29, doi:10.1039/c8tb02629g (2019).

6 Tong, R., Chen, G., Tian, J. & He, M. Highly Stretchable, Strain-Sensitive, and Ionic-Conductive Cellulose-Based Hydrogels for Wearable Sensors. *Polymers (Basel)* **11**, 11122067, doi:10.3390/polym11122067 (2019).

7 Tong, R. *et al.* Stretchable and sensitive sodium alginate ionic hydrogel fibers for flexible strain sensors. *Int. J. Biol. Macromol.* **246**, 125683, doi:10.1016/j.ijbiomac.2023.125683 (2023).

8 Wu, J. *et al.* Multiply cross-linked poly(vinyl alcohol)/cellulose nanofiber composite ionic conductive hydrogels for strain sensors. *Int. J. Biol. Macromol.* **225**, 1119-1128, doi:10.1016/j.ijbiomac.2022.11.173 (2023).